Published in final edited form as:
Oral Oncol. 2014 February ; 50(2): 104–112. doi:10.1016/j.oraloncology.2013.10.014.

Silencing Met receptor tyrosine kinase signaling decreased oral tumor growth and increased survival of nude mice

X. Tao[a], **K.S. Hill**[a], **I. Gaziova**[a], **S.K. Sastry**[b,e], **S. Qui**[c,e], **P. Szaniszlo**[d], **S. Fennewald**[d], **V.A. Resto**[d,e], and **L.A. Elferink**[a,e,*]

[a] Department of Neuroscience and Cell Biology, University of Texas Medical Branch, Galveston, TX 77555-1074, United States

[b] Department of Biochemistry and Molecular Biology, University of Texas Medical Branch, Galveston, TX 77555-1074, United States

[c] Department of Pathology, University of Texas Medical Branch, Galveston, TX 77555-1074, United States

[d] Department of Otolaryngology, University of Texas Medical Branch, Galveston, TX 77555-1074, United States

[e] Department of Sealy Center for Cancer Biology, University of Texas Medical Branch, Galveston, TX 77555-1074, United States

SUMMARY

Objectives—The hepatocyte growth factor receptor (Met) is frequently overexpressed in Head and Neck Squamous Cell Carcinoma (HNSCC), correlating positively with high-grade tumors and shortened patient survival. As such, Met may represent an important therapeutic target. The purpose of this study was to explore the role of Met signaling for HNSCC growth and locoregional dissemination.

Materials and methods—Using a lentiviral system for RNA interference, we knocked down Met in established HNSCC cell lines that express high levels of the endogenous receptor. The effect of Met silencing on in vitro proliferation, cell survival and migration was examined using western analysis, immunohisto-chemistry and live cell imaging. *In vivo* tumor growth, dissemination and mouse survival was assessed using an orthotopic tongue mouse model for HNSCC.

Results—We show that Met knockdown (1) impaired activation of downstream MAPK signaling; (2) reduced cell viability and anchorage independent growth; (3) abrogated HGF-

*Corresponding author. Current address: Department of Neuroscience and Cell Biology, University of Texas Medical Branch, Galveston, 301 University Blvd, TX 77555-1074, United States. Tel.: +1 409 772 2775; fax: +1 409 747 1938. lisa.elferink@utmb.edu (L.A. Elferink)..

Conflict of interest statement
The authors declare no conflict of interests.

Appendix A. Supplementary material
Supplementary data associated with this article can be found, in the online version, at http://dx.doi.org/10.1016/j.oraloncology.2013.10.014.

induced cell motility on laminin; (4) reduced *In vivo* tumor growth by increased cell apoptosis; (5) caused reduced incidence of tumor dissemination to regional lymph nodes and (6) increased the survival of nude mice with orthotopic xenografts.

Conclusion—Met signaling is important for HNSCC growth and locoregional dissemination *In vivo* and that targeting Met may be an important strategy for therapy.

Keywords

MET; HGF receptor; Head and neck squamous cell carcinoma; Oral cancer; Tumorigenesis

Introduction

Despite current multimodal therapies, the 5-year survival rate for patients with head and neck cancers remains low making it the 5th leading cause of cancer by incidence and the 6th leading cause of cancer mortality in the world [1–3]. Over 90% of head and neck malignancies are squamous cell carcinoma (HNSCC), originating from the epithelial lining of the oral cavity, oropharynx, hypopharynx and larynx [4]. Although these tumors arise from different anatomical sites, they appear histologically identical, share some etiological risk factors and overlapping metastatic sites [4]. HNSCC vary significantly in their human papillomavirus (HPV) status, in particular the HPV16 genotype [5,6]. Of note HPV16 status is recognized as a good prognostic factor in HNSCC, as HPV16 positive patients show significantly higher survival rates to radiotherapy when compared to HPV16 negative patients [7].

Overexpression of receptor tyrosine kinases is a common feature of several cancers, particularly HNSCC. Upregulation of the Epidermal Growth Factor Receptor (EGFR) is a signature event in 90% of HNSCC and functions as a strong indicator for poor patient survival, radioresistance and locoregional failure [8–11]. When combined with cytotoxic chemotherapeutics, EGFR-targeted therapeutics have shown promising efficacies for the treatment of HNSCC [12,13]. Unfortunately, acquired resistance to EGFR therapeutics and recurrence is a common outcome in clinical trials [14,15]. Thus, there is an urgent need for an increased understanding of additional signaling pathways important for HNSCC growth and survival.

Binding of Hepatocyte Growth Factor (HGF) to its target receptor tyrosine kinase Met promotes cell proliferation, survival and motility cellular responses that could afford HNSCCs a selective advantage for growth and/or survival [16,17]. Met expression is increased and functional in 90% of HNSCC cell lines and 84% of patient samples [18,19]. Notably, increased Met levels in HNSCC patients correlate closely with an aggressive clinical phenotype of these cancers including increased regional dissemination, recurrence and decreased disease-free survival [20,21]. Recently, the Met receptor was reported to contribute to erlotinib resistance in HNSCC cells [15]. Moreover, dual blockage of Met and EGFR abrogated the proliferation and growth of HNSCC cells *in vitro* and tumor xenografts *In vivo*, relative to EGFR inhibition only [15] reinforcing an important role for Met signaling in HNSCC. However the precise contribution of Met signaling in the growth and

dissemination of HNSCC, particularly in the microenvironment of the oral cavity remains unclear.

In the present study we sought to further investigate the contribution of Met signaling for HNSCC growth and dissemination using an orthotopic mouse model for HNSCC. Here we show that treatment with the Met inhibitor SU11274 blocked cell motility in response to HGF. Similarly Met knockdown (MetKD) using short hairpin RNA (shRNA) in HNSCC cells lines reduced cell motility and anchorage-independent growth *in vitro*. Moreover, we report that shRNA-mediated depletion of Met extended the survival of mice, correlating with reduced tumor burden and dissemination to lymph nodes, decreased cell proliferation and increased tumor cell apoptosis. Our findings indicate an important role for Met signaling for HNSCC growth and survival within the oral cavity, loco-regional dissemination and survival.

Materials and methods

Reagents and antibodies

All general reagents were obtained from Fisher Scientific or Sigma–Aldrich unless indicated otherwise. SU11274 was purchased from Calbiochem Inc. Antibodies used for immunoblotting and immunoprecipitation were c-MET C28 (Santa Cruz Biotechnology), phospho-Met Tyr-1234, Tyr-1235 (UpState Biotechnology), Phospho p42/p44 and p42/p44 MAPK (Cell Signaling Technology), anti-β-actin (Sigma–Aldrich), Transferrin Receptor (TfR) (Zymed Laboratories), anti-mouse HGF and anti-mouse HGFR antibody (R&D Systems), goat IgG (Jackson ImmunoResearch Laboratories), peroxidase-conjugated goat anti-rabbit and goat anti-mouse secondary antibody (Jackson ImmunoResearch Laboratories). Antibodies for immunohistochemistry were anti-human HGFR (R&D Systems), anti-mouse HGF (LifeSpan Biosciences), Ki67 (Cell Signaling Technology), cleaved caspase-3 (Abcam), biotinylated anti-rabbit and anti-goat secondary antibodies (Vector laboratories). Human and mouse recombinant HGF were purchased from Pepro-Tech Inc.

Cell lines, RT-PCR analysis, flow cytometry, shRNA and transfection

JHU-SCC-011, JHU-SCC-012 and JHU-SCC-019 cells have been described elsewhere [22–24]. Cells were maintained in RPMI medium 1640 (Gibco life technologies) with 10% Fetal Bovine Serum (FBS) and 1x Penicillin/Streptomycin. Genomic DNA isolated from JHU-SCC-011, JHU-SCC-012 and JHU-SCC-019 cells was HPV genotyped for HPV types 16, 18, 31 and 33 using RT-PCR as previously described [25]. Recombinant lentivirus encoding the shRNA METKD-2 (5′-CGGAGACTCATAATCCAACTGTAACTCGAGTTACAGTTGGATTATGAGTCTTTTTTG-3′),METKD-1 (5′CCGGGCACTATTATAGGACTTGTATCTCGAGATACAAGTCTTATAATAGTGCTTTTG-3′) or non-targeting (NT) control shRNA (5′CTAAGGTTAAGTCGCCCTCGCTCGAGCGAGGGCGACTTAACCTTAGG-3′) were prepared and used to infect JHU-SCC-012 and JHU-SCC-019 cells, as previously described [26]. Stable MetKD cells were selected in the presence of 5 μg/mL puromycin for 7 days and colonies maintained in

media containing 1 μg/mL puromycin for 2 months and Met surface levels screened using flow cytometry [22].

HGF ELISA assays were performed as previously described [26,27]. Anchorage independent growth assays, human HGF ELISA, cell scatter and wound healing assays have been described elsewhere [22]. Live cell imaging was performed as previously described [22] with the exception that serum-depleted cells (1% FBS) were plated at a density of 2×10^5 cells on 35 mm glass bottom tissue culture plates pre-coated with 15 μg/mL laminin (Sigma Aldrich) overnight at 4 °C prior to imaging.

Cell viability

Cell viability assay was performed using 96-well plates and the CellTiter-Blue cell viability assay kit (Promega). 1500 cells/well of JHU-SCC-012 or 2000 cells/well of JHU-SCC-019 MetKD or NT cells in 100 μL culture medium were plated on 96-well plate and grown for 24 h. Cells were serum starved with 1%FBS in RPMI medium for another 24 h, then treated with 100 ng/mL HGF. Media supplemented with HGF were changed every day. For each time point, 20 μL of CellTiter-Blue solution was added to each well, plates were incubated at 5% CO_2, 37 °C for 4 h and fluorescence read 560/590 nm using a spectrofluorometer (Spectra Max Gemini XS, Molecular Devices, Sunnyvale, CA). The values represent the means ± SE from three microwells. Experiments were repeated 3 times.

Immunoprecipitation and western blot analysis

For western blot, cell lysates were prepared in TGH buffer (50 mM Hepes, pH 7.4, 150 mM NaCl, 1.5 mM $MgCl_2$, 1 mM ethylene glycol tetraacetic acid (EGTA), pH 8.0, 1% Triton X100, 10% glycerol, 1 μg/mL BSA), containing protease inhibitors (2 μg/mL aprotinin, 2 μg/mL leupeptin, 2 μg/mL pepstatin A, Phenylmethanesulfonyl fluoride, phosphatase inhibitors (10 mM NaF, 2 mM Na_3VO_4). Western analysis performed using ChemiGlow substrate (Proteinsimple). For immunoprecipitations, mouse tongues were homogenized in radioimmune precipitation assay buffer (150 mM NaCl, 50 mM Tris pH 7.4, 0.1% SDS, 1% Nonidet P-40, 0.5% sodium deoxycholate), containing protease inhibitors, centrifuged at 15,000*g* for 5 min and the supernatants were collected. 1000 μg of each supernatant was incubated with 1 μg of HGFR antibody (R&D Systems) overnight at 4 °C. Antibody-protein complexes were precipitated using 50 μL of protein A/G-agarose solution (Pierce) by rotation at 4 °C for 4 h. The protein-beads complex were collected by centrifugation at 1000g for 5 min, washed with lysis buffer 3 times, resuspended in SDS loading buffer and fractionated by SDS/PAGE.

Orthotopic tumor studies

Four week-old athymic nude mice (Charles River Laboratories) were housed in specific pathogen free conditions. JHU-SCC-012, JHU-SCC-019, immortalized oral keratinocytes (OKF-TERT1) (1×10^6 cells in 50 lL sterile PBS) or PBS as a negative control, were each injected into the mobile lateral tongues of nude mice ($n = 5$ per sample). Mice were euthanized once they exhibited 20% weight loss or at the 6 months post-injection time point. To study the effect of MetKD *In vivo*, stable MetKD or NT control cells (1×10^5 suspended in 50 μL of sterile PBS) were orthotopically injected into the mobile lateral tongue ($n = 5$ per

sample), and mice were sacrificed at 30 days post injection. Tongues were fixed in 4% paraformaldehyde in PBS at 4 °C. Five-micrometer-thick sections were prepared. Animal care was in strict compliance with the institutional guidelines established at the University of Texas Medical Branch.

Haematoxylin eosin (H&E) and immunohistochemistry staining

Slides were deparaffinized with xylene prior to rehydration with ethanol. All slides were counterstained with hematoxylin then blinded so that two individuals performed scoring in an unbiased manner. Tumor area was measured in um^2 on H&E stained sections using Zeiss AxioScope A1 (Oberkochen, Germany) and analyzed using AxioVision software (Zeiss). Immunohistochemistry was performed using adjacent sections as described elsewhere [22]. The number of positive (CP) and negative (CN) cells were counted and the% positive staining (%P) was determined using the equation: %P = (CP/(CP + CN)) 100 and are reported as the mean ± S.E.

Statistical analysis

All statistical analyses were performed using GraphPad Prism software (v4), using a One or Two-way analysis of variance (ANOVA) with a Bonferroni post hoc analysis to determine statistical significance between groups.

Results

Paracrine activation of MET signaling functions in HNSCC cells

We first examined Met levels in normal tissue and HNSCCs derived from human tongue. As expected, immunohistochemistry confirmed high Met protein levels in all human HNSCC tumors, consistent with a previous report [20]. High Met expression was also detected in the epithelial layer of adjacent normal mucosa in all cases, consistent with the highly proliferative capacity of this tissue (Fig. 1a). We next examined Met expression in the HNSCC cell lines JHU-SCC-012 and JHU-SCC-019 cells. RT-PCR analysis showed that both cell lines are negative for the HPV genotypes 16, 18, 31 and 33 (data not shown). JHU-SCC-012 tested wild type for the tumor suppressor p53 whereas JHUSCC-019 cells are mutant for p53 [28], a key mutation in 65% of HNSCC that is associated with poor overall patient survival [29]. Western analysis confirmed Met expression in the HNSCC lines JHU-SCC-012 and JHU-SCC-019 cells. Phosphorylation of Met (on two key tyrosine residues, Y1234/Y1235) as well as the downstream target ERK was detected only in response to HGF (Fig. 1b). Sequence analysis confirmed that endogenous Met in these cell lines is wild type and does not harbor oncogenic mutations implicated in other cancer types (data not shown). Comparable results were detected using the HNSCC line JHU-SCC-011 (data not shown), a cell line that expresses mutant p53 [28] and is HPV negative (data not shown). ELISA detected no HGF in conditioned media collected from these cells (Fig. 1c), confirming a paracrine mechanism for Met activation in these lines. U87 glioblastoma cells served as a positive control for HGF secretion under these conditions [27].

The tumor microenvironment is critical for the survival and proliferation of HNSCCs at primary and metastatic sites [30–32]. Therefore, we examined whether mouse tongue and

cervical lymph nodes would provide a source of HGF for Met-mediated cell growth. Immunoprecipitation and western analysis confirmed the expression of Met and HGF in mouse tongue (Fig. 2a). Immunohistochemistry confirmed HGF staining in mouse tongue and cervical lymph nodes (Supplemental Fig. 1). Cross species differences in the interaction of murine HGF (mHGF) with human Met has been reported [26,33,34]. Using conditions that result in maximal Met phosphorylation by human HGF, western analysis confirmed that human Met was phosphorylated on residues Y1234/Y1235 by mHGF using site specific phospho-tyrosine antibodies (Fig. 2b). As expected, treatment with mHGF resulted in the phosphorylation of downstream ERK under these conditions. Given these findings, we orthotopically injected JHU-SCC-012 and JHU-SCC-019 cells into the mobile lateral tongues of nude mice. Nude mice injected with saline or immortalized oral keratinocytes (OKF-TERT1) served as controls. Mice injected with saline or OKF-TERT1 cells failed to form tumors as assessed by necropsy 6 months post-injection. This is in contrast to mice injected with JHU-SCC-012 or JHU-SCC-019 cells which formed tumors quickly and succumbed at 11.3 ± 1.1, 14.4 ± 3.3 (mean ± SEM) days post injection respectively (Fig. 2c). H&E staining of fixed tissues revealed that JHU-SCC-012 and JHUSCC-019 cells readily formed tumors in tongues at the site of injection. Histologic characterization of the established tumors revealed an invasive phenotype for the primary tumors (Supplemental Fig. 2). Moreover metastatic tumors in cervical lymph nodes were readily detected in animals injected with JHU-SCC-012 or JHU-SCC-019 cells (Fig. 2d). Evaluation of the lymph node specimens revealed a highly invasive phenotype that was disruptive of lymph node architecture (Supplemental Fig. 2). No tumor was identified in examined lung tissue (not shown).

Pharmacological inhibition of Met reduces HNSCC cell motility in vitro

Met signaling has been shown to promote cell motility in many different cell types. Given the invasive phenotype of the orthotopic tumors derived from JHU-SCC-012 and JHU-SCC-019 cells, we examined the importance of Met for cell motility using cell scatter and wound healing assays. As shown, treatment with HGF induced scattering of JHU-SCC-012 (Fig. 3a) and JHU-SCC-019 (Fig. 3b), a phenotype that was abrogated by pre-incubation of the cells with 2.5 uM of SU11274 for 30 min, a tyrosine kinase inhibitor for Met. Consistent with this data, wound healing as-says revealed that pre-treatment of cells with SU11274 reversed the stimulatory effect of HGF on JHU-SCC-012 and JHU-SCC-019 cells motility in (Fig. 3c and d respectively). Western analysis confirmed inhibition of Met phosphorylation by SU11274 under these conditions (Supplemental Fig. 3).

Knockdown of Met in HNSCCs

Since SU11274 is not amenable to use *In vivo*, we employed an RNA interference strategy using two different Met specific shRNA sequences (MetKD1 and MetKD2) to knockdown Met (MetKD) expression in JHU-SCC-019 and JHU-SCC-012 cells. We were unable to generate a stable population of JHU-SCC-012 MetKD cells using shRNA 1 but obtained transient knockdown with shRNA 2, suggesting that Met may be a critical regulator of cell survival or proliferation in this line. Conversely, JHU-SCC-019 MetKD cells were viable. Western analysis confirmed stable knockdown of total and phosphorylated Met following HGF treatment in JHU-SCC-019 and JHU-SCC-012 MetKD cells relative to control cells

expressing a non-targeting (NT) shRNA (Fig. 4a and b). As expected, lower levels of HGF-stimulated pERK were detected in MetKD cells when compared to NT expressing cells. Flow cytometry analysis confirmed reduced expression of cell surface Met in JHU-SCC-012 and JHUSCC-019 MetKD cells compared to control NT cells (Fig. 4c and d).

To assess the effect of Met signaling on the tumorigenic potential of JHU-SCC-012 and JHU-SCC-019 cells, we performed anchorage independent growth assays in soft agar. NT and MetKD cells were seeded into 0.4% agarose in the presence or absence of HGF and the number of resulting colonies (defined as a cluster of three or more cells) was scored. In NT cell lines, HGF treatment resulted in a significant increase in the number of colonies present in soft agar consistent with a role for Met signaling in anchorage independent cell growth. Conversely, HGF-treated MetKD cells showed reduced capacity for anchorage independent growth (Fig. 5a and b). Consistent with a role for Met signaling in cell survival, MetKD cells showed a significant reduction in cell viability when compared to NT control (Fig. 5c and d).

We next examined the effect of MET knockdown on HNSCC cell motility. As shown in Fig. 6a and b, JHU-SCC-012 and JHU-SCC-019 MetKD cells showed reduced HGF-induced motility compared to NT cells using wound healing assays (Supplemental Fig. 4), consistent with our earlier studies using treatment with SU11274 to block Met signaling. We previously reported the JHU-SCC-019 cells show a strong preference for binding to laminin [22], one of several extracellular matrix components identified in lymph nodes. As a result, we performed live cell imaging studies to measure differences in HGF-induced migration of JHU-SCC-019 NT and MetKD cell lines seeded on laminin. Cells were allowed to adhere for 1 h on laminin prior to treatment with HGF, after which live cell migration was examined by measuring the total path length of migrating cells over a 2 h period. In the absence of HGF, comparable migratory path lengths and velocities were detected for JHUSCC-019 MetKD and NT cells (NT, 191.0 μm ± 25.6 and MetKD, 189.7 μm ± 20.7; NT, 1.59 μm/min ± 0.21 and MetKD, 1.58 μm/min ± 0.17) (Fig. 6c). Treatment with HGF increased the path length of NT cells (297.0 μm ± 16.2), correlating closely with increased cell velocity (2.84 μm/min ± 0.14) (Fig. 6c and d). Conversely, no increase in MetKD cell path length or velocity was observed following HGF treatment (157.6 μm ± 21.8 and 1.31 μm/min ± 0.18 respectively) (Supplemental Fig. 5). The differences in cell migration are unlikely the result of differences in cell-laminin interactions as NT and MetKD express comparable levels of cell surface Integrin β1 (Supplemental Fig. 5C).

Knockdown of Met signaling suppresses tumor growth, cell proliferation and increases cell apoptosis In vivo

The effect of Met knockdown on JHU-SCC-012 and JHU-SCC-019 cell viability, motility and anchorage independent growth were directly comparable. Since JHU-SCC-012 cells were not amenable to stable MetKD, we used the JHU-SCC-019 MetKD cell lines in our orthotopic tongue model to examine the role of Met signaling for primary HNSCC growth and regional dissemination. We first examined the survival of nude mice following orthotopic injection with equal numbers of MetKD versus NT control cells. Survival rate was examined every day for up to 75 days. As shown in Fig. 7a, the survival rate was

significantly higher in mice injected with MetKD cells compared to control mice at 50 days. Given these findings, we examined the effect of MetKD on tumor growth and regional dissemination 30 days post-injection. Tongues and cervical lymph nodes from orthotopically injected mice were removed and processed for histologic and immunohistochemical analysis. Regional dissemination to the cervical lymph nodes was not detected in mice injected with MetKD cells compared to mice injected with NT cells (Fig. 7b). Morphometric analysis of H&E stained tongue sections show a significant reduction in the size of primary tumors derived from MetKD cells compared to mice injected with NT cells (Fig. 7c). Immunohistochemistry confirmed strong Met staining in the primary tumors derived from NT cells and not JHU-SCC-019 MetKD tumors (Fig. 7d). Notably, tumors derived from MetKD cells show decreased cell proliferation as indicated by reduced Ki67 staining (Fig. 7e) with elevated cell apoptosis as indicated by increased cleaved caspase 3 (CCP3) staining (Fig. 7f). These results indicate an important role for Met signaling in HNSCC growth and/or survival *In vivo*.

Discussion

Despite considerable advances in surgical techniques and adjuvant therapeutics for treating HNSCC, the high rate of recurrence coupled with the tendency for acquired resistance to EGFR-targeted therapies underscores the importance of identifying additional pathways important for HNSCC survival and dissemination [4]. Thus the need for an increased understanding of additional molecular mechanisms as points of clinical intervention remains urgent. Here we report that knockdown of the Met receptor tyro-sine kinase using shRNA is associated with decreased cell proliferation, viability and migration on laminin *in vitro*. *In vivo*, Met knockdown resulted in decreased tumor burden and dissemination to cervical lymph nodes using an orthotopic tongue model, correlating with reduced cell proliferation and an increased apoptotic index. Notably, Met knockdown significantly increased the survival of nude mice with orthotopic xenografts. Thus our data support a role for Met as a valid therapeutic target for HNSCC intervention.

Our findings using RNA interference are consistent with previous pharmacological studies, suggesting that Met may be a suitable clinical target for the treatment of HNSCC. Met antagonism using the pharmacological inhibitor PF2341066 caused a significant decrease in primary tumor burden in a subcutaneous xenograft mouse model using UM-22B cells, correlating with decreased cell proliferation and increased apoptosis [20]. Interestingly, a parallel study using 686LN cells reported negligible differences in tumor volume following treatment with the Met inhibitor PF04217903 relative to the control group [15]. Met signaling has also been implicated in acquired resistance of HNSCC to EGFR-targeted therapies. For example dual blockage with the EGFR and Met inhibitors gefitinib and PF2341066 respectively, reduced the volume of tumor xenografts significantly suggesting cross-talk between these signaling pathways [35]. Consistent with this, a novel mechanism of erlotinib resistance in a HNSCC line that over expressed the non receptor tyrosine kinase c-Src, involved Met signaling [15]. Interestingly, these cells were not resistant to the EGFR inhibitor cetuximab. Although the reasons for these discrepancies remain unclear, it may reflect differences in the oncogenic dependency of HNSCC cells for Met signaling. Several molecules that target the Met receptor pathway in solid tumors notably NSCLC are in phase

I and II clinical trials and show promising results. A phase II clinical study (NCT00725764) using the inhibitor GSK1363089 (formerly XL880) in adults with HNSCC has been completed, although the results are not yet available.

Notably, we present the first evidence that stable knockdown of Met in orthotopic head and neck tumors decreased dissemination to cervical nodes and increased the survival of mice relative to the control group. Our preclinical findings are significant in that lymph node dissemination is a key clinical feature of HNSCC that is most predictive of mortality [36,37]. Evidence of neck lymphatic spread is an accepted prognostic factor for HNSCC, characterizing the primary tumor as clinically aggressive, often less responsive to therapy correlating with poor patient survival. Given the well-documented role of Met signaling for promoting the growth, survival and invasiveness of malignant cells, how could Met signaling contribute to nodal dissemination in our orthotopic model? We cannot rule out the possibility that reduced lymph node dissemination may reflect the smaller size of the primary tumors routinely produced by MetKD cells. We recently reported that JHU-SCC-019 cells bind laminin, a key extracellular matrix component within the lymph node parenchyma component, under low fluid shear conditions [22]. Our data indicating that MetKD does not alter cell-laminin adhesion, but does reduce HGF-induced cell motility on this substrate may suggest that the process of HNSCC lodgment within lymph nodes is not dependent on Met signaling. Rather, Met signaling may confer an advantage for HNSCC survival in this unique microenvironment. Consistent with this hypothesis, we show that cervical lymph nodes in mice serve as a rich source of HGF. Additionally, HGF has been shown to protect HNSCC cell lines from cellular apoptosis following loss of contact with the extracellular matrix (anoikis) [38]. In a highly invasive HNSCC line, Met signaling enhanced the activity of matrix metalloproteinase-9 and urokinase-type plasminogen activator, enzymes that degrade the extracellular matrix and facilitate cell migration and invasion [39]. Although Met overexpression is evident at all tumor stages, increased Met staining is significantly increased in HNSCC patients associated with enlarged or multiple (N2-N3) lymph node metastasis [40,41] and locoregional recurrence [42]. Additionally, increased levels of HGF have been reported in HNSCC patients when compared to healthy individuals [43]. Thus Met signaling may enhance HNSCC spread to cervical lymph node through multiple mechanisms including increased cell growth and/or survival.

Conventional HNSCC can be categorized into two prognostic and therapeutic groups – HPV-negative tumors that are associated with an aggressive phenotype and HPV-positive HNSCC, which are highly predictive for lymph node metastasis [44–46]. The prevalence of HPV among all HNSCCs varies between 21.95% and 40.3% depending on the anatomical site of the primary tumors and patient etiologies [46]. Our finding that MET knockdown in the HPV-negative JHU-SCC-019 cell line reduced cervical lymph node spread and increased survival of mice in an orthotopic animal model is novel and significant. Future studies focused on understanding the role of Met signaling in HPV-positive HNSCCs seems likely to provide additional new insights into the therapeutic value of targeting Met in the treatment of different HNSCC subtypes.

Supplementary Material

Refer to Web version on PubMed Central for supplementary material.

Acknowledgments

We thank members of the Elferink laboratory for helpful comments and John Helms in the UTMB Cancer Center for assistance with figures. This work was supported in part by funding from the NIH: CA119075 (L.E.), CA118405 (S.S.) and CA-132988 (V.R.).

References

1. Parkin DM, Bray F, Ferlay J, Pisani P. Global cancer statistics, 2002. CA Cancer J Clin. 2005; 55(2):74–108. [PubMed: 15761078]
2. Siegel R, Naishadham D, Jemal A. Cancer statistics, 2013. CA Cancer J Clin. 2013; 63(1):11–30. [PubMed: 23335087]
3. Chen AY, DeSantis C, Jemal A. US mortality rates for oral cavity and pharyngeal cancer by educational attainment. Arch Otolaryngol Head Neck Surg. 2011; 137(11):1094–9. [PubMed: 22106232]
4. Leemans CR, Braakhuis BJ, Brakenhoff RH. The molecular biology of head and neck cancer. Nat Rev Cancer. 2011; 11(1):9–22. [PubMed: 21160525]
5. Price KA, Cohen EE. Current treatment options for metastatic head and neck cancer. Curr Treat Options Oncol. 2012; 13(1):35–46. [PubMed: 22252884]
6. Lleras RA, Smith RV, Adrien LR, et al. Unique DNA methylation loci distinguish anatomic site and HPV status in head and neck squamous cell carcinoma. Clin Cancer Res. 2013:12. [PubMed: 23172882]
7. Thibaudeau E, Fortin B, Coutlee F, et al. HPV prevalence and prognostic value in a prospective cohort of 255 patients with locally advanced HNSCC: a single-centre experience. Int J Otolaryngol. 2013; 2013:437815. [PubMed: 23710185]
8. Bleijerveld OB, Brakenhoff RH, Schaaij-Visser TB, et al. Protein signatures associated with tumor cell dissemination in head and neck cancer. J Proteomics. 2011; 74(4):558–66. [PubMed: 21262401]
9. Choi P, Jordan CD, Mendez E, et al. Examination of oral cancer biomarkers by tissue microarray analysis. Arch Otolaryngol Head Neck Surg. May; 2008 134(5):539–46. [PubMed: 18490578]
10. Chung CH, Parker JS, Karaca G, et al. Molecular classification of head and neck squamous cell carcinomas using patterns of gene expression. Cancer Cell. 2004; 5(5):489–500. [PubMed: 15144956]
11. Chung CH, Zhang Q, Hammond EM, et al. Integrating epidermal growth factor receptor assay with clinical parameters improves risk classification for relapse and survival in head-and-neck squamous cell carcinoma. Int J Radiat Oncol Biol Phys. 2011; 81(2):331–8. [PubMed: 20732768]
12. Saarilahti K, Bono P, Kajanti M, et al. Phase II prospective trial of gefitinib given concurrently with cisplatin and radiotherapy in patients with locally advanced head and neck cancer. J Otolaryngol – Head Neck Surg = Le J d'oto-rhinolaryngologie et de chirurgie cervico-faciale. 2010; 39(3):269–76.
13. Sano D, Matsumoto F, Valdecanas DR, et al. Vandetanib restores head and neck squamous cell carcinoma cells' sensitivity to cisplatin and radiation in vivo and in vitro. Clin Cancer Res. 2011; 17(7):1815–27. [PubMed: 21350000]
14. Brand TM, Iida M, Wheeler DL. Molecular mechanisms of resistance to the EGFR monoclonal antibody cetuximab. Cancer Biol Ther. 2011; 11(9):777–92. [PubMed: 21293176]
15. Stabile LP, He G, Lui VW, et al. C-Src activation mediates erlotinib resistance in head and neck cancer by stimulating c-Met. Clin Cancer Res. 2013; 19(2):380–92. [PubMed: 23213056]
16. Birchmeier C, Birchmeier W, Gherardi E, Vande Woude GF. Met, metastasis, motility and more. Nat Rev Mol Cell Biol. 2003; 4(12):915–25. [PubMed: 14685170]

17. Gherardi E, Birchmeier W, Birchmeier C, Vande Woude G. Targeting MET in cancer: rationale and progress. Nat Rev Cancer. 2012; 12(2):89–103. [PubMed: 22270953]
18. Seiwert TY, Jagadeeswaran R, Faoro L, et al. The MET receptor tyrosine kinase is a potential novel therapeutic target for head and neck squamous cell carcinoma. Cancer Res. 2009; 69(7): 3021–31. [PubMed: 19318576]
19. De Herdt MJ, Baatenburg de Jong RJ. HGF and c-MET as potential orchestrators of invasive growth in head and neck squamous cell carcinoma. Front Biosci. 2008; 13:2516–26. [PubMed: 17981731]
20. Knowles LM, Stabile LP, Egloff AM, et al. HGF and c-Met participate in paracrine tumorigenic pathways in head and neck squamous cell cancer. Clin Cancer Res. 2009; 15(11):3740–50. [PubMed: 19470725]
21. Lo Muzio L, Farina A, Rubini C, et al. Effect of c-Met expression on survival in head and neck squamous cell carcinoma. Tumour Biol. 2006; 27(3):115–21. [PubMed: 16612144]
22. Fennewald SM, Kantara C, Sastry SK, Resto VA. Laminin interactions with head and neck cancer cells under low fluid shear conditions lead to integrin activation and binding. J Biol Chem. 2012; 287(25):21058–66. [PubMed: 22547070]
23. Rocco JW, Leong CO, Kuperwasser N, DeYoung MP, Ellisen LW. P63 mediates survival in squamous cell carcinoma by suppression of p73-dependent apoptosis. Cancer Cell. Jan; 2006 9(1): 45–56. [PubMed: 16413471]
24. Scher RL, Koch WM, Richtsmeier WJ. Induction of the intercellular adhesion molecule (ICAM-1) on squamous cell carcinoma by interferon gamma. Arch Otolaryngol Head Neck Surg. 1993; 119(4):432–8. [PubMed: 8096142]
25. Cattani P, Zannoni GF, Ricci C, et al. Clinical performance of human papillomavirus E6 and E7 mRNA testing for high-grade lesions of the cervix. J Clin Microbiol. 2009; 47(12):3895–901. [PubMed: 19828739]
26. Hill KS, Gaziova I, Harrigal L, et al. Met receptor tyrosine kinase signaling induces secretion of the angiogenic chemokine interleukin-8/CXCL8 in pancreatic cancer. PLoS ONE. 2012; 7(7):e40420. [PubMed: 22815748]
27. Garnett J, Chumbalkar V, Vaillant B, et al. Regulation of HGF expression by DeltaEGFR-mediated c-Met activation in glioblastoma cells. Neoplasia. Jan; 2013 15(1):73–84. [PubMed: 23359207]
28. Hoque MO, Begum S, Sommer M, et al. PUMA in head and neck cancer. Cancer Lett. 2003; 199(1):75–81. [PubMed: 12963126]
29. Lindenbergh-van der Plas M, Brakenhoff RH, Kuik DJ, et al. Prognostic significance of truncating TP53 mutations in head and neck squamous cell carcinoma. Clin Cancer Res. 2011; 17(11):3733–41. [PubMed: 21467160]
30. Swartz MA, Lund AW. Lymphatic and interstitial flow in the tumour microenvironment: linking mechanobiology with immunity. Nat Rev Cancer. 2012; 12(3):210–9. [PubMed: 22362216]
31. Swartz MA, Iida N, Roberts EW, et al. Tumor microenvironment complexity: emerging roles in cancer therapy. Cancer Res. 2012; 72(10):2473–80. [PubMed: 22414581]
32. Vered M, Dayan D, Salo T. The role of the tumour microenvironment in the biology of head and neck cancer: lessons from mobile tongue cancer. Nat Rev Cancer. 2011; 11(5):382. author reply 382. [PubMed: 21455256]
33. Yokoi K, Kim SJ, Thaker P, et al. Induction of apoptosis in tumor-associated endothelial cells and therapy of orthotopic human pancreatic carcinoma in nude mice. Neoplasia. 2005; 7(7):696–704. [PubMed: 16026649]
34. Zhang YW, Su Y, Volpert OV, Vande Woude GF. Hepatocyte growth factor/scatter factor mediates angiogenesis through positive VEGF and negative thrombospondin 1 regulation. Proc Natl Acad Sci U S A. 2003; 100(22):12718–23. [PubMed: 14555767]
35. Xu H, Stabile LP, Gubish CT, Gooding WE, Grandis JR, Siegfried JM. Dual blockade of EGFR and c-Met abrogates redundant signaling and proliferation in head and neck carcinoma cells. Clin Cancer Res. 2011; 17(13):4425–38. [PubMed: 21622718]

36. Goldson TM, Han Y, Knight KB, Weiss HL, Resto VA. Clinicopathological predictors of lymphatic metastasis in HNSCC: implications for molecular mechanisms of metastatic disease. J Exp Ther Oncol. 2010; 8(3):211–21. [PubMed: 20734920]
37. Olsen KD, Caruso M, Foote RL, et al. Primary head and neck cancer. Histopathologic predictors of recurrence after neck dissection in patients with lymph node involvement. Arch Otolaryngol Head Neck Surg. 1994; 120(12):1370–4. [PubMed: 7980903]
38. Lau PC, Chan AT. Novel therapeutic target for head and neck squamous cell carcinoma: HGF-MET signaling pathway. Anti-Cancer Drugs. 2011; 22(7):665–73. [PubMed: 21709616]
39. Lim YC, Park HY, Hwang HS, et al. (-)-Epigallocatechin-3-gallate (EGCG) inhibits HGF-induced invasion and metastasis in hypopharyngeal carcinoma cells. Cancer Lett. 2008; 271(1):140–52. [PubMed: 18632202]
40. Cortesina G, Martone T, Galeazzi E, et al. Staging of head and neck squamous cell carcinoma using the MET oncogene product as marker of tumor cells in lymph node metastases. Int J Cancer. 2000; 89(3):286–92. [PubMed: 10861506]
41. Galeazzi E, Olivero M, Gervasio FC, et al. Detection of MET oncogene/hepatocyte growth factor receptor in lymph node metastases from head and neck squamous cell carcinomas. Eur Arch Otorhinolaryngol. 1997; 254(Suppl 1):S138–43. [PubMed: 9065649]
42. de Carvalho AC, Kowalski LP, Campos AH, Soares FA, Carvalho AL, Vettore AL. Clinical significance of molecular alterations in histologically negative surgical margins of head and neck cancer patients. Oral Oncol. 2012; 48(3):240–8. [PubMed: 22104250]
43. Di Renzo MF, Olivero M, Martone T, et al. Somatic mutations of the MET oncogene are selected during metastatic spread of human HNSC carcinomas. Oncogene. 2000; 19(12):1547–55. [PubMed: 10734314]
44. Mendelsohn AH, Lai CK, Shintaku IP, et al. Histopathologic findings of HPV and p16 positive HNSCC. The Laryngoscope. 2010; 120(9):1788–94. [PubMed: 20803740]
45. Hoffmann M, Gorogh T, Gottschlich S, et al. Human papillomaviruses in head and neck cancer: 8 year-survival-analysis of 73 patients. Cancer Lett. 2005; 218(2):199–206. [PubMed: 15670897]
46. Dayyani F, Etzel CJ, Liu M, Ho CH, Lippman SM, Tsao AS. Meta-analysis of the impact of human papillomavirus (HPV) on cancer risk and overall survival in head and neck squamous cell carcinomas (HNSCC). Head Neck Oncol. 2010; 2:15. [PubMed: 20587061]

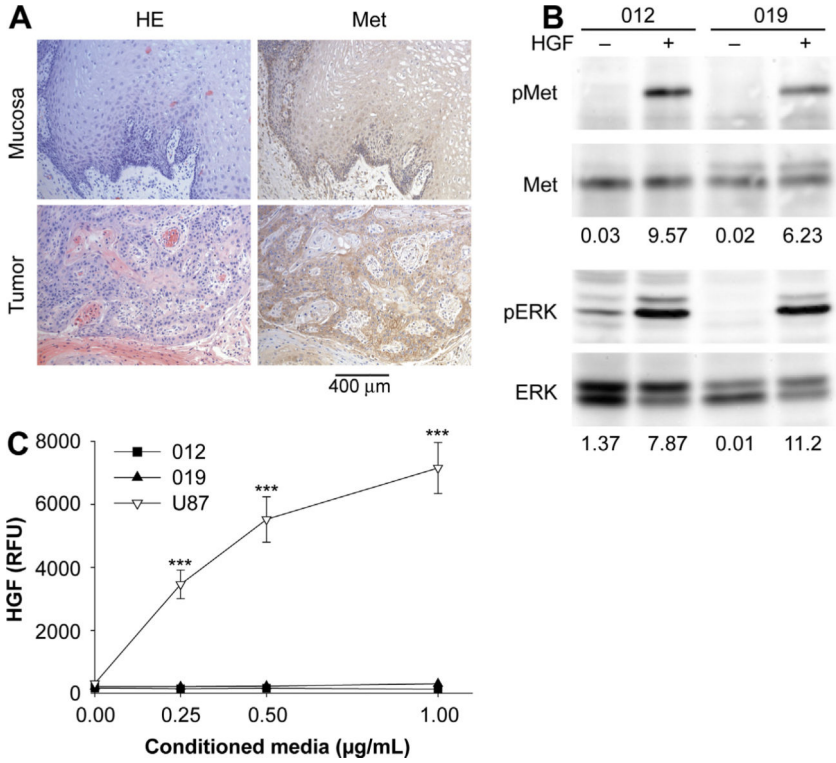

Figure 1.

Met signaling in human oral cancer. (A) H&E staining and Met immunohistochemistry revealed that human oral tumor cells express higher levels of Met compared to adjacent normal mucosa ($n = 5$). (B) Lysates from JHU-SCC-012 or JHU-SCC-019 cells treated without (−) or with (+) 100 ng/mL HGF for 5 min were examined by western analysis for Met, ERK and phosphorylation of Met (pMet, Y1234/1235) and ERK (pERK). Representative results from triplicate experiments are shown. The relative density of pMet/Met and pERK/ERK is indicated beneath the respective blots. (C) HGF-ELISA detected no HGF in conditioned media from JHU-SCC-012 and JHU-SCC-019 cells whereas U87 cells were positive for HGF secretion. Values are expressed as the average mode ± SEM (*** $p < 0.001$; ANOVA) from triplicate experiments.

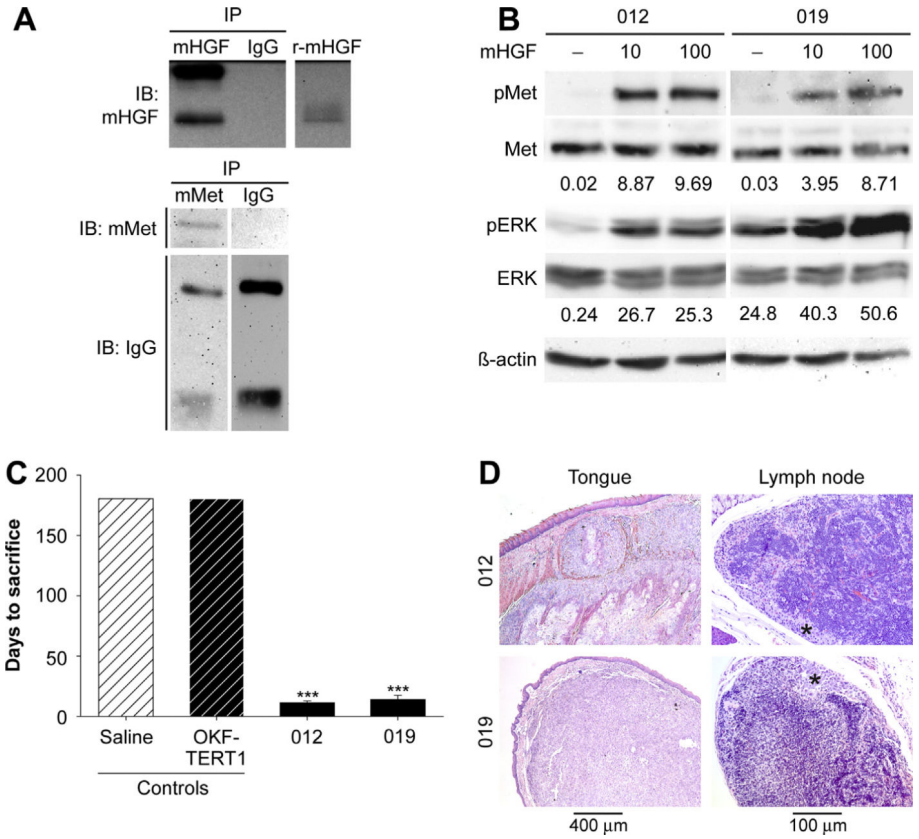

Figure 2.

Human HNSCCs form orthotopic tumors in mice. (A) Western analysis of immunoprecipitations from mouse tongue lysates using antibodies for mouse HGF (mHGF), mouse Met (mMet) or goat IgG detected mHGF (top panel) and mMet (lower panel) is this tissue. Recombinant mouse HGF (r-mHGF) was used as positive control. Representative results from triplicate experiments are shown. (B) Sera starved JHU-SCC-012 and JHU-SCC-019 cells were treated without (−) or with 10 ng/mL or 100 ng/mL HGF and examined by western analysis for pMet, Met pERK, ERK and β-actin. Representative results from triplicate experiments are shown. The relative density of pMet/Met of pERK/ERK compared to β-actin is shown beneath the respective blots. (C) Mean survival of mice ($n = 5$) injected orthotopically into the lateral tongue with saline, immortalized oral keratinocytes (OKF-TERT1), JHU-SCC-012 or JHU-SCC-019 cells (1×10^6). Values are expressed as the average mode ± SEM (*** $p < 0.001$; ANOVA) of triplicate experiments. The graph represents days to sacrifice at the end of protocol (6 months) or following 20% weight loss. (D) Histological analysis of tumor bearing mice by H&E staining of the tongue and lymph node. Asterisks denotes tumor in lymph node.

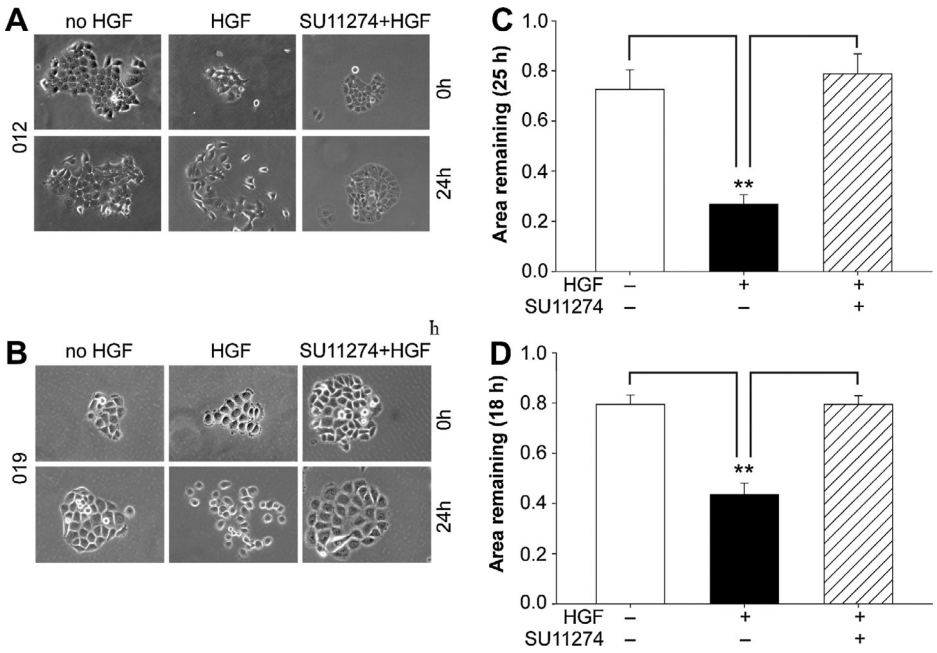

Figure 3.

Pharmacological inhibition of Met reduces cell motility. Cell scatter responses of JHU-SCC-012 (A) or JHU-SCC-019 (B) cells treated with (+) or without (−) HGF and/or SU11274 as indicated. Representative images from triplicate experiments are shown. Wound healing assays were performed using JHU-SCC-012 (C) or JHU-SCC-019 (D) cells as indicated and are reported as the area remaining at each time point (18 or 25 h) following HGF treatment (0 h) (Anova, ** $p < 0.01$) of triplicate experiments.

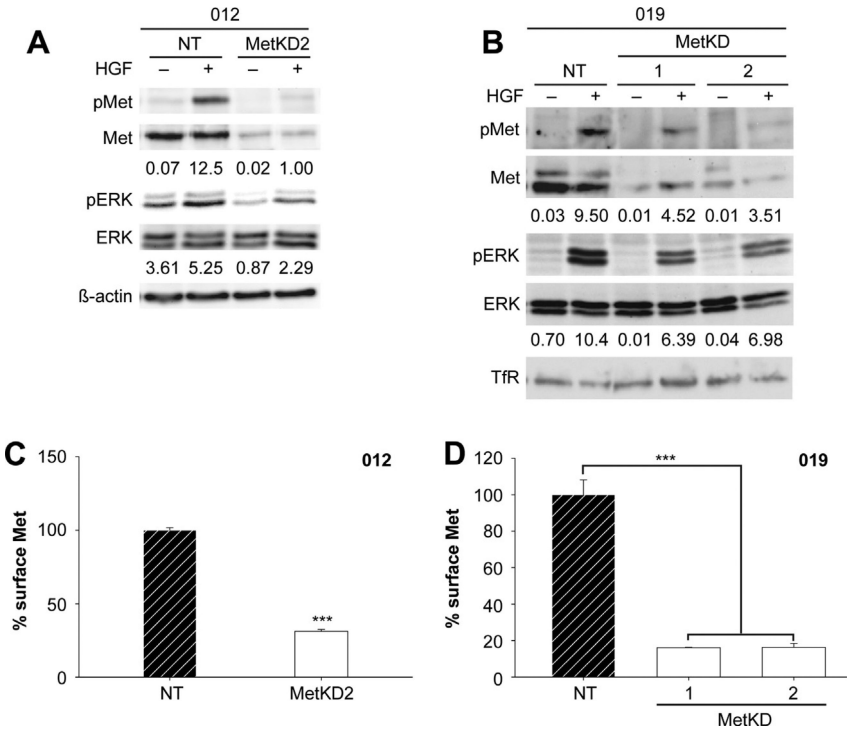

Figure 4.

Met knockdown in JHU-SCC-012 and JHU-SCC-019 cells. JHU-SCC-012 (A) or JHU-SCC-019 (B) cells infected with recombinant lentivirus expressing Met knockdown shRNA (1 or 2) or a non-targeting (NT) shRNA were treated without (−) or with (+) HGF and examined by Western analysis for pMet (Y1234/1235), Met, pERK, ERK, β-actin or Transferrin Receptor (TfR) levels. Representative results from triplicate experiments are shown. The relative density of pMet/Met of pERK/ERK compared to β-actin or TfR is shown beneath the respective blots. Flow cytometry detected reduced cell surface Met levels in JHU-SCC-012 (C) and JHU-SCC-019 MetKD (D) cell lines. Values are expressed as the average mode ± SEM (*** $p < 0.001$; ANOVA) of three independent experiments.

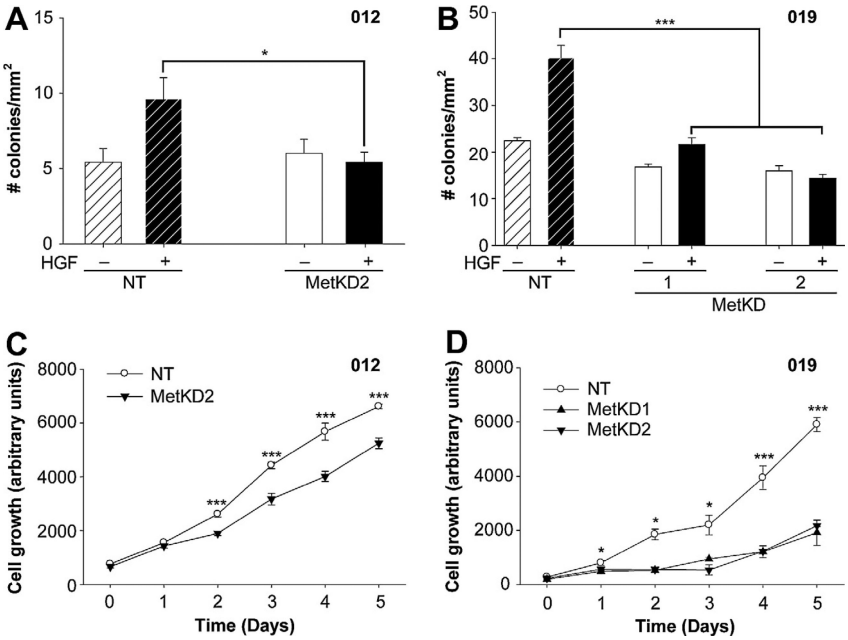

Figure 5.

Decreased cell motility, viability and anchorage-independent growth in response to MetKD. Reduced anchorage-independent growth of JHU-SCC-012 (A) and JHUSCC-019 (B) MetKD cells in soft agar (* $p < 0.05$, *** $p < 0.001$, ANOVA) in triplicate experiments. MetKD reduced the growth of JHU-SCC-012 (C) and JHU-SCC-019 (D) cells relative to NT controls (*** $p < 0.001$, * $p < 0.05$, ANOVA, $n = 3$) of three independent experiments.

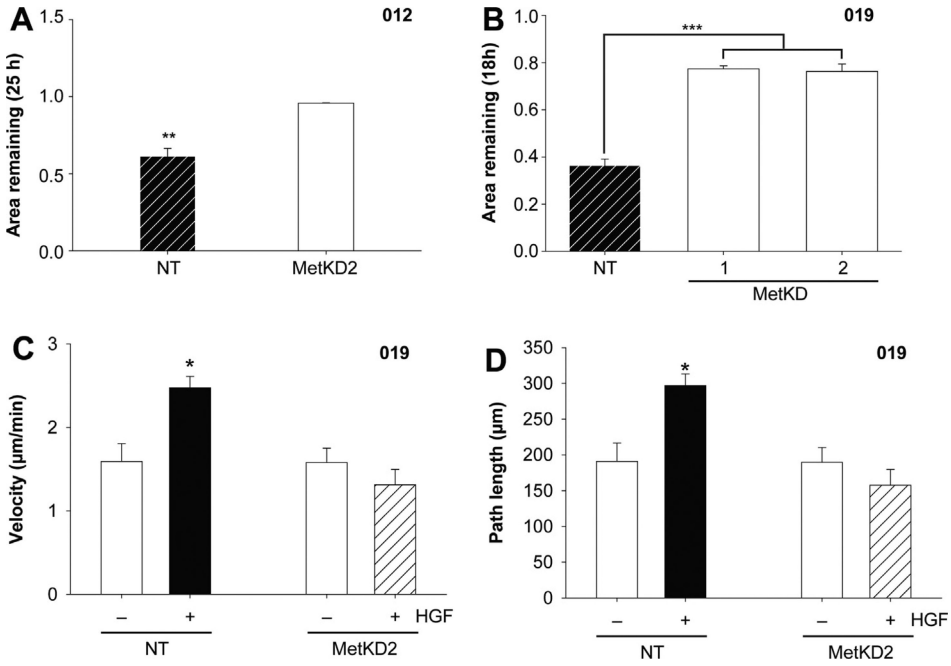

Figure 6.

MetKD reduced cell motility of JHU-SCC-012 and JHU-SCC-019 cells. HGF induced wound closure is decreased in JHU-SCC-012 (A) and JHU-SCC-019 MetKD (B) cells relative to NT cells (** $p < 0.01$, *** $p < 0.001$, ANOVA, $n = 3$). Live cell imaging of JUH-SCC-019 MetKD cells plated on laminin-coated glass bottom cell culture dishes show decreased cell velocity (C) and path length (D) in response to 100 ng/mL HGF. Images were collected every 2 min for a total of 120 min and the data is expressed as the mean path length ± SEM per condition (*** $p < 0.001$; ANOVA, $n > 30$ cells) of duplicate experiments. Representative images are shown.

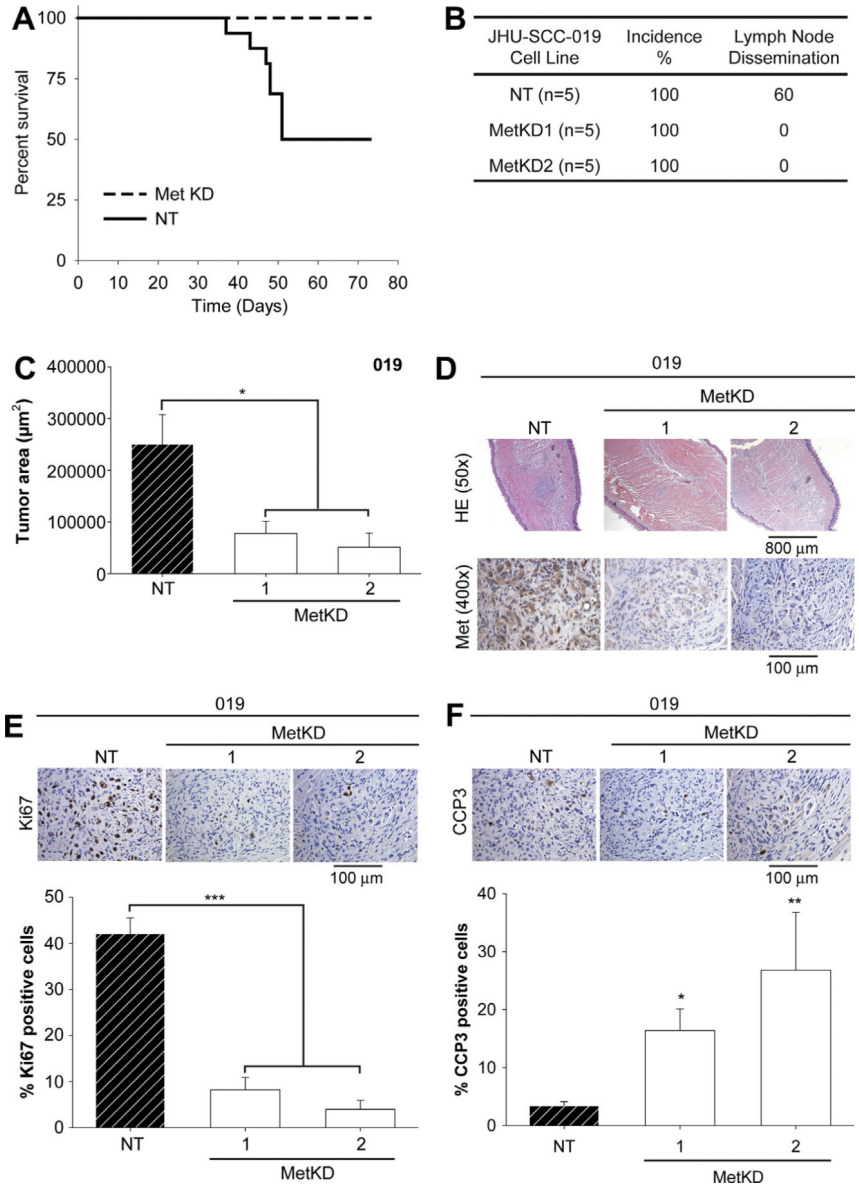

Figure 7.

Reduced tumor burden *In vivo* following MetKD. Mice were injected orthotopically into the lateral tongue with JHU-SCC-019 MetKD ($n = 5$) or control (NT) cells ($n = 5$). Survival rates were examined every day for up to 75 days and are plotted as a Kaplan Meier curve (A). 30 days post injection, serial sections of paraffin-embedded tongues and cervical lymph nodes were H&E stained and analyzed for tumor dissemination (B) and size (C). Adjacent slides were processed for Met (D), Ki67 (E) and cleaved caspase 3 (CCP3) (F) staining. Morphometric analysis indicated a significant decrease in tumor size and Ki67 staining with increased CCP3 per high powered field in MetKD-derived versus NT-derived tumors (* $p < 0.05$, ** $p < 0.01$, *** $p < 0.001$; ANOVA, $n = 5$). Representative images are shown.